SIGNAL PROCESSING ISSUES IN INDOOR POSITIONING BY ULTRA WIDE BAND RADIO AIDED INERTIAL NAVIGATION

John-Olof Nilsson[1◇], *Alessio De Angelis*[2], *Isaac Skog*[1], *Paolo Carbone*[2], *and Peter Händel*[1]

[1]Signal Processing Lab, ACCESS Linnaeus Centre, Royal Institute of Technology, Stockholm, Sweden, ◇jnil02@kth.se
[2]Department of Electronic and Information Engineering, University of Perugia, Italy

ABSTRACT

The difficulties and possibilities connected to indoor positioning suggest using several sources of navigational information. Apart from the signal processing of the individual sources this gives rise to the need for information fusion. This article aims at presenting and describing the signal processing methods and issues faced when constructing a navigation system based on a local ultra wide band (UWB) ranging system and an inertial navigation system (INS). The signal processing methods within the individual systems are described together with techniques for fusing the information from them. Finally, filtering results of experimental data is presented with expected convergence properties and positioning accuracy of below ± 4 *cm.*

1. INTRODUCTION

The applications in which indoor positioning information is critical or beneficial are numerous, efficient travelling, industrial automation, and cargo handling to mention a few. However, in comparison with an outdoor environment, an indoor environment adds several limitations and difficulties as well as possibilities for a positioning system. For example, the nature of the environment, including many obstacles and narrow passages, requires high accuracy. Further, an indoor environment often has an attenuated global positioning system (GPS) signal making the GPS, the current paradigm of radio navigation, difficult to use. On the other hand, the limited extent and controlled nature of the indoor environment adds the possibility of external infrastructure and several studies show the feasibility of using local radio positioning system for indoor positioning [1][2][3]. However, apart from attenuating the GPS signal, the structures and infrastructures enclosing and traversing the indoor environment will disturb and attenuate the radio signal used by the local radio positioning system as well. Thus, additional sources providing complementary navigational information are desirable. Finally, the nature of many of the applications, for which an indoor positioning system would be aimed, puts limitations on the size and the cost of the system.

Exploring the possibilities of a radio based local indoor positioning system, a low cost navigation system based on a UWB radio ranging system and an INS, was built. A system level presentation of the system can be found in [4].

Apart from the signal processing of the individual signals, using two sources of navigational information adds the issue of fusing the information in a sensible manner. This article aims at presenting the signal processing and information fusion methods and issues faced when designing and implementing the system.

The outline of the article is as follows. In Section 2 the individual systems, the UWB radio ranging system and the INS, are presented. In Section 3 the method of fusing the navigational information from the two systems is described. In Section 4 experimental results are presented.

1.1 Notation

Vector quantities are denoted with boldface letters, e.g. $\mathbf{x}$, and matrix quantities are denoted with capital boldface letters, e.g. $\mathbf{P}$. The scalar k is used as time index. Estimated states will be indicated with a circumflex, e.g. $\hat{\mathbf{x}}_k$, while measured quantities will be indicated with a tilde, e.g. $\tilde{z}_{l,k}$. $\mathbf{0}$ and $\mathbf{I}$ will be used to denote zero vectors and matrices, and identity matrices, of indicated sizes. The symbol $\equiv$ will be used when new quantities are defined from old ones. The symbols $:=$ will be used when variables are assigned new values. The euclidean-2-norm will be written as $|\cdot|$. The transpose of a vector or matrix is indicated with superscripted T.

2. NAVIGATION SYSTEM

The navigation system consists of two complementary subsystems, a UWB radio ranging system and an INS. Further, the system can be divided into a user part, the navigation unit, consisting of an inertial measurement unit (IMU) and a UWB master unit together with a PC, and an infrastructure part consisting of UWB slave units of known location in the operation area. The UWB radio ranging system works by measuring the distance between the master unit and the slave units, see Section 2.1, while the INS uses the IMU, providing measurement of linear acceleration and angular rates, to propagate mechanisation equations to obtain estimates of navigational states, see Section 2.2. The propagation of the mechanisation equations as well as the information fusion is performed on the PC.

2.1 Ultra wide band radio ranging system

The UWB radio ranging system measures distance between a master unit and a slave unit by measuring the round trip time (RTT) of a UWB radio pulse. The logical circuit architecture of the master and the slave unit is based on the system presented in [5] while the UWB radio pulse generator is based on the step recovery diode design presented in [6].

In short, the master unit activates a slave unit by transmitting a unique slave identity code. Upon receiving the identity code the slave unit will switch into an echo mode for a fixed time period during which, after a fixed time delay, it will answer each received UWB radio pulse with another UWB radio pulse generating a “round trip”. After sending the identity code the master transmits a series of pulses. After each pulse it listens for the retransmitted pulse and measures the

RTT with an analogue power detector and a time-to-digital converter. After the fixed time period in the echo mode the slave will exit the mode and again start listening for its identity code and the master can activate another unit. While a specific unit is activated, all the others are in a disabled state for the same fixed time period.

Ideally, with infinite bandwidth and no measurement noise, the RTT-to-distance relation should read

$$t_{\text{RTT}} = \frac{2 \cdot z_l}{c} + t_{0,\text{master}} + t_{0,\text{slave}_l}$$

where t_{RTT} is the RTT, z_l the distance between master and slave unit l, c the speed of light, and $t_{0,master}$ and t_{0,slave_l} the delays introduced by the hardware in the master and slave unit, respectively. However, as explained in [5], due to limited bandwidth and measurement noise, the true RTT-to-distance relation shows an approximately linear (depending on pulse shape) relation but with a slightly higher slope k_{RTT}, which has to be determined by calibration. Also, the hardware time delays, $t_{0,master}$ and t_{0,slave_l}, are due to component manufacturing tolerances, detector threshold level, and unknown inter-equipment signal path, i.e. cabling length, not known beforehand. However, since only one master unit was available they had to be determined in pairs, i.e. $t_{0,l} \equiv t_{0,master} + t_{0,slave_l}$, for each slave unit l. Finally adding a measurement noise term n_0, scaled by k_{RTT}, whose variance, due to limited bandwidth and free space path loss, is dependent on RTT, gives the RTT-to-distance relation

$$t_{\text{RTT}} = k_{\text{RTT}} \cdot z_l + t_{0,l} + n_0 \cdot k_{\text{RTT}},$$

for slave l and distance z_l, and solving for the distance

$$z_l = \frac{t_{\text{RTT}} - t_{0,l}}{k_{\text{RTT}}} + n_0.$$

Further, as explained in Section 3, to correctly combine the distance measurement with the INS, the covariance of the measurement noise as a function of RTT had to be determined. Based on calibration data an exponential function was found to describe the observed covariance well,

$$R = \text{cov}(n_0, n_0) = \sigma_0^2 \exp(k_{\sigma^2} z_l). \tag{1}$$

As shown in [4] the range measurements can be used by themselves to estimate position and velocity by using a tracking filter, but here only using the unfiltered distance measurements to support the INS will be treated. However, note that, even though the distance measurements can be used to infer the position, they contain little information about orientation. Also, the mere dependence on position (as in contrast to the inertial measurements which depend on the second derivative of position, acceleration) and the slow update rate (10 Hz) give a poor dynamic range.

2.2 Inertial navigation

The INS can be divided into a sensor part (the IMU), and a computational part. In our case the IMU is an Inertia-Link® from MicroStrain®. The IMU contains temperature compensated MEMS triaxial accelerometer and gyroscope. The computational part is implemented on a PC to which the IMU is connected.

The navigational states are collected in a state vector $\mathbf{x}$, composed of subvectors of position $\mathbf{r}$, velocity $\mathbf{v}$, and attitude θ, all in three dimensions,

$$\mathbf{x}_{nav} = [\mathbf{r} \quad \mathbf{v} \quad \theta]^{\text{T}},$$

while the linear acceleration $\mathbf{a}$, and the angular velocity ω, in three dimensions alike, are collected in a system input vector $\mathbf{u}$,

$$\mathbf{u} = [\mathbf{a} \quad \omega]^{\text{T}}.$$

The navigational states, driven by the linear acceleration and angular velocity, propagate according to some nonlinear differential equation,

$$\dot{\mathbf{x}}_{nav}(t) = f_{nav}\big(\mathbf{x}_{nav}(t), \mathbf{u}(t)\big),$$

and the measured linear acceleration and angular velocity $\tilde{\mathbf{u}}_k$, are functions of the true linear acceleration and angular velocity $\mathbf{u}_k$, sensor states , temperature, time, etc, plus a measurement noise $\mathbf{n}_{1,k}$,

$$\tilde{\mathbf{u}}_k = f_{meas}(\mathbf{u}_k, \dots) + \mathbf{n}_{1,k}.$$

Assuming the dominant contribution of $f_{meas}(\cdot)$ to be an addition of bias terms (more sensor states could easily be added to the system), the measurements are modelled as

$$\tilde{\mathbf{u}}_k = \mathbf{u}_k - \mathbf{b}_k + \mathbf{n}_{1,k}$$

where $\mathbf{b}$ is composed of slowly varying accelerometer biases $\mathbf{b}_a$ and gyroscope biases $\mathbf{b}_\omega$,

$$\mathbf{b} = [\mathbf{b}_a \quad \mathbf{b}_\omega]^{\text{T}}.$$

The variation (drift) of the bias terms is assumed to be driven by some stochastic zero mean noise. Finally, appending the bias terms to the navigational states,

$$\mathbf{x} = [\mathbf{x}_{nav} \quad \mathbf{b}]^{\text{T}},$$

and using a discrete approximation of $f_{nav}(\cdot)$ the full state vector $\mathbf{x}$, are assumed to propagate according to a difference equation

$$\mathbf{x}_{k+1} = f_{ins}(\mathbf{x}_k, \tilde{\mathbf{u}}_k) + \mathbf{n}_{2,k}$$

where the noise term $\mathbf{n}_{2,k}$, describs the deviation from the ideal $f_{nav}(\cdot)$, caused by measurement noise and model approximation and discretization errors, and the slow drift in the bias states. The noise term is assumed zero mean.

Given an initial estimate of the system states, $\hat{\mathbf{x}}_0$, and inertial measurements, $\tilde{\mathbf{u}}_k$, the INS can give estimates of the system states for all k by propagating the estimates according to

$$\hat{\mathbf{x}}_{k+1} = f_{ins}(\hat{\mathbf{x}}_k, \tilde{\mathbf{u}}_k). \tag{2}$$

However, since the IMU in use has a strapdown configuration of the individual sensors, the measurements will be done in a sensor frame different from the navigation frame. Further, according to the equivalence principle, the gravitational acceleration will be indistinguishable from a true acceleration and hence must be compensated for. This means that the propagation of the mechanization equations will have to be performed in several steps. With the current estimate of orientation the measurement will first have to be transformed into the navigation frame. After this a gravity model

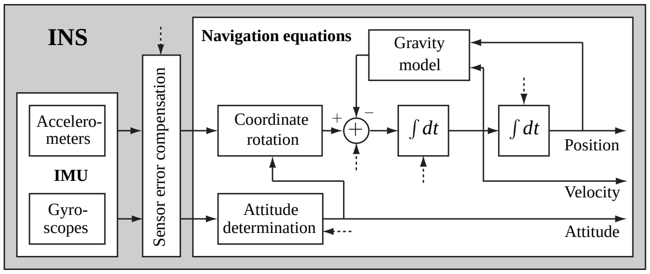

Figure 1: Conceptional diagram of a strap-down INS. The dash arrows indicate points for insertion of calibration (aiding) data.

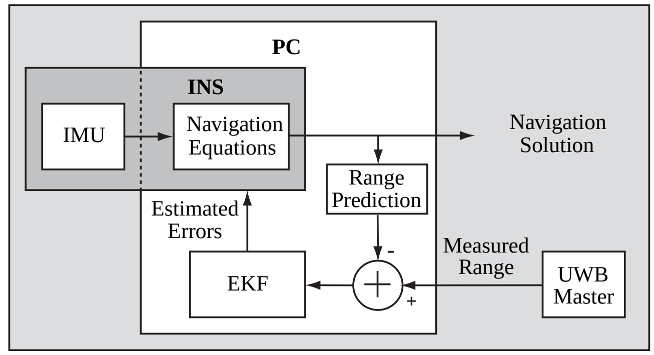

Figure 2: Conceptional diagram of the information fusion.

is used to compensate for the gravitational acceleration, and finally the accelerometer and gyroscope measurements are integrated to achieve position, velocity, and attitude. As for the bias states, which are assumed driven by a white noise (random walk), their propagation according to equation (2) will only be identity. A block diagram description of the INS and hence the effect of equation (2), can be seen in Figure 1. Detailed description of common implementations of (2) can be found in standard inertial navigation litterature [7][8].

As described above, the INS is selfcontained and with the correct state initialization capable of giving estimates (relative to the initial values) of a complete set of navigational states (position, velocity, and attitude) for infinite time. Inertial measurements can be done at high rates (in the present system 100Hz), which together with the fact that they correspond to the second and first derivative of position and orientation, gives a high dynamic range, and they are essentially immune to external disturbances. However, due to the integrative nature of the INS, amplifying low frequency noise, and the low performance solid state sensors in use, the errors will swiftly grow beyond acceptable levels after only a few seconds of stand alone use.

3. INFORMATION FUSION

As noted, the INS will have unbounded errors and only relative navigational information while the UWB range measurements do not provide attitude information and give a poor dynamic range. By combining these two systems we can compensate for these shortcomings and obtain better navigational information than from any individual system. This is done with a range aided INS architecture.

In short, as shown in the illustration of the system in Figure 2, in the range aided INS architecture the INS provides the main navigational system. Hence, the extended Kalman filter (EKF) does not directly estimate the INS states but instead estimates the error in the INS states based on the discrepancy of the estimated range, calculated from the estimated INS states, and the range measured by the UWB radio ranging system. The estimated errors are then fed back to the INS for correction of its states. The advantage of this structure in comparison with a tracking filter is that the computationally costly covariance update is done at the lower pace of the range measurement and that the number of states is reduced since acceleration and angular velocity are not estimated. Also, it allows for a modular setup since the INS is left more or less untouched.

3.1 Error model

Given an estimation of the INS state $\hat{\mathbf{x}}_k$, define error states as

$$\delta\mathbf{x}_k \equiv \mathbf{x}_k - \hat{\mathbf{x}}_k.$$

From the mechanisation equations (2) and the above definition a discrete approximation of the differential equation describing the propagation of the error states is found,

$$\delta\mathbf{x}_{k+1} = f_{err}(\delta\mathbf{x}_k, \mathbf{x}_k, \tilde{\mathbf{u}}_k) + \mathbf{n}_{3,k}.$$

Derivation of error equations in various coordinate systems can be found in [7][8].

3.2 Range error

To utilize the EKF structure the range measurements need to be related to the error states. From the knowledge of the position $\mathbf{r}_{\text{slave}_l}$ of the UWB slave unit l, to which we refer the current range measurement, and our true and estimated positions, $\hat{\mathbf{r}}_k$ and $\mathbf{r}_k$, a range and a range prediction are defined and calculated as

$$z_{l,k} \equiv |\mathbf{r}_{\text{slave}_l} - \mathbf{r}_k| \quad \text{and} \quad \hat{z}_{l,k} = |\mathbf{r}_{\text{slave}_l} - \hat{\mathbf{r}}_k|.$$

In accordance with previous error definitions the error in the range prediction $\delta z_{l,k}$ and the measured error in the range prediction $\delta\tilde{z}_{l,k}$ are defined as

$$\delta z_{l,k} \equiv z_{l,k} - \hat{z}_{l,k} \quad \text{and} \quad \delta\tilde{z}_{l,k} \equiv \tilde{z}_{l,k} - \hat{z}_{l,k}.$$

The measured range is assumed to relate to the true range via an additive measurement noise,

$$\tilde{z}_{l,k} = z_{l,k} + n_{4,k},$$

and therefore so is the measured error in the range prediction to the true error in range prediction,

$$\delta\tilde{z}_{l,k} = \tilde{z}_{l,k} - \hat{z}_{l,k} = z_{l,k} + n_{4,k} - \hat{z}_{l,k} = \delta z_{l,k} + n_{4,k}.$$

To spell it out we have

$$\begin{aligned}\delta\tilde{z}_{l,k} &= \delta z_{l,k} + n_{4,k} = z_{l,k} - \hat{z}_{l,k} + n_{4,k} \\ &= |\mathbf{r}_{\text{slave}_l} - \mathbf{r}_k| - |\mathbf{r}_{\text{slave}_l} - \hat{\mathbf{r}}_k| + n_{4,k} \\ &= |\mathbf{r}_{\text{slave}_l} - (\delta\mathbf{r}_k + \hat{\mathbf{r}}_k)| - |\mathbf{r}_{\text{slave}_l} - \hat{\mathbf{r}}_k| + n_{4,k} \\ &= h_{l,k}(\delta\mathbf{x}_k) + n_{4,k}\end{aligned}$$

where we have defined the measurement function, $h_{l,k}(\cdot)$, as

$$h_{l,k}(\delta\mathbf{x}_k) \equiv |\mathbf{r}_{\text{slave}_l} - (\delta\mathbf{r}_k + \hat{\mathbf{r}}_k)| - |\mathbf{r}_{\text{slave}_l} - \hat{\mathbf{r}}_k|.$$

3.3 Error estimation

The filtering consists of two phases, prediction and update. In the prediction phase the state estimations and the estimation error covariances are propagated. However, since it is the error states we are estimating, any nonzero estimation should be fed back to the INS. Naturally it turns out that

$$f_{err}(\mathbf{0}_{15\times1}, \mathbf{x}_k, \tilde{\mathbf{u}}_k) = \mathbf{0}_{15\times1}$$

and hence once the estimated error states are fed back to the INS (and therefore set to zero) they will remain identical to zero throughout the prediction phase. In other words, the feedback loop saves us from having to propagate the error states and from the prediction phase perspective $\delta\hat{\mathbf{x}}_k = 0$ for all k. This does not hold true for the estimation error covariances,

$$\mathbf{P}_k = \mathrm{cov}\big((\delta\mathbf{x}_k - \delta\hat{\mathbf{x}}_k), (\delta\mathbf{x}_k - \delta\hat{\mathbf{x}}_k)\big),$$

which propagate as

$$\mathbf{P}_{k+1} = \mathbf{F}_k\mathbf{P}_k\mathbf{F}_k^{\mathrm{T}} + \mathbf{Q}_k$$

where

$$\mathbf{F}_k = \left.\frac{\partial f_{err}}{\partial \delta\mathbf{x}}\right|_{\delta\hat{\mathbf{x}}_k, \tilde{\mathbf{u}}_k} \quad \text{and} \quad \mathbf{Q}_k = \mathrm{cov}(\mathbf{n}_{3,k}, \mathbf{n}_{3,k}).$$

Now, as soon as a range measurement is available, the filter will enter the update phase in which the error states are updated with the new knowledge that the range measurement adds. As described in Section 3.2 a range prediction is calculated and the measured error in the range prediction is formed. The new information in the measured range prediction error is in the innovation y_k, see below. However, because of the feedback loop $\delta\hat{\mathbf{x}}_k = \mathbf{0}_{15\times1}$, giving $h_{l,k}(\delta\hat{\mathbf{x}}_k) = 0$, and therefore the innovation is the measured error in the range prediction itself,

$$y_k = \delta\tilde{z}_k - \overbrace{h_{l,k}(\delta\hat{\mathbf{x}}_k)}^{=0} = \delta\tilde{z}_k.$$

Further, to update the error state estimation, the Kalman gain, $\mathbf{K}_{l,k}$, is needed, which depends on the observation matrix,

$$\mathbf{H}_{l,k} = \left.\frac{\partial h_l}{\partial \delta\mathbf{x}}\right|_{\delta\hat{\mathbf{x}}_k}.$$

Once again $\delta\hat{\mathbf{x}}_k = 0$ and therefore

$$\mathbf{H}_{l,k} = \begin{bmatrix} \frac{\hat{r}_{x,k} - r_{x,\mathrm{slave}_l}}{|\mathbf{r}_{\mathrm{slave}_l} - \hat{\mathbf{r}}_k|} & \frac{\hat{r}_{y,k} - r_{y,\mathrm{slave}_l}}{|\mathbf{r}_{\mathrm{slave}_l} - \hat{\mathbf{r}}_k|} & \frac{\hat{r}_{z,k} - r_{z,\mathrm{slave}_l}}{|\mathbf{r}_{\mathrm{slave}_l} - \hat{\mathbf{r}}_k|} & \mathbf{0}_{1\times12} \end{bmatrix} \quad (3)$$

and together with the estimation error covariance the Kalman gain is calculated as

$$\mathbf{K}_{l,k} = \mathbf{P}_k\mathbf{H}_{l,k}^{\mathrm{T}}(\mathbf{H}_{l,k}\mathbf{P}_k\mathbf{H}_{l,k}^{\mathrm{T}} + R_k)^{-1}$$

where R_k comes from equation (1).

Thus, when a range measurement is available, the error states are updated as

$$\begin{aligned} \delta\hat{\mathbf{x}}_k &:= \overbrace{\delta\hat{\mathbf{x}}_k}^{=\mathbf{0}_{15\times1}} + \mathbf{K}_{l,k}y_k \\ &= \mathbf{K}_{l,k}\big(\delta\tilde{z}_{l,k} - \overbrace{h_{l,k}(\delta\hat{\mathbf{x}}_k^-)}^{=0}\big) \\ &= \mathbf{K}_{l,k}(\tilde{z}_{l,k} - |\mathbf{r}_{\mathrm{slave}_l} - \hat{\mathbf{r}}_k|), \end{aligned}$$

and hence also the estimation error covariances have to be updated,

$$\mathbf{P}_k := (\mathbf{I}_{15\times15} - \mathbf{K}_{l,k}\mathbf{H}_{l,k})\mathbf{P}_k.$$

Finally, the estimated error states are fed back to the INS, which also necessarily sets the estimated error states to zero,

$$\hat{\mathbf{x}}_k := \hat{\mathbf{x}}_k + \delta\hat{\mathbf{x}}_k \quad \Rightarrow \quad \delta\hat{\mathbf{x}}_k := \mathbf{0}_{15\times1}.$$

To start the INS and the information fusion, the INS states, the error states, and the estimation error covariances need to be initialized, i.e. $\hat{\mathbf{x}}_0$, $\delta\hat{\mathbf{x}}_0$, and $\mathbf{P}_0$ set. However, due to the feedback loop the system is not sensitive to this and will normally converge as long as the values are within the right order of magnitude.

A summary of the information fusion algorithm can be found in Table 1. Details on and motivation for the Kalman filter can be found in standard estimation literature, e.g. [9].

Table 1: Summary of the signal processing algorithm in the UWB radio range aided INS navigation system.

$\hat{\mathbf{x}}_0 := \mathbf{x}_{init}$, $\mathbf{P}_0 := \mathbf{P}_{init}$, $\delta\hat{\mathbf{x}}_0 := \mathbf{0}_{15\times1}$
loop k
  if $\tilde{z}_{l,k}$ exist : l
    $\mathbf{H}_{l,k} =$ (see (3)), $R_k =$ (see (1))
    $\mathbf{K}_{l,k} = \mathbf{P}_k\mathbf{H}_{l,k}^{\mathrm{T}}(\mathbf{H}_{l,k}\mathbf{P}_k\mathbf{H}_{l,k}^{\mathrm{T}} + R_k)^{-1}$
    $\delta\hat{\mathbf{x}}_k = \mathbf{K}_{l,k}(\tilde{z}_{l,k} - |\mathbf{r}_{\mathrm{slave}_l} - \hat{\mathbf{r}}_k|)$
    $\mathbf{P}_k := (\mathbf{I}_{15\times15} - \mathbf{K}_{l,k}\mathbf{H}_k)\mathbf{P}_k$
    $\hat{\mathbf{x}}_k := \hat{\mathbf{x}}_k + \delta\hat{\mathbf{x}}_k$, $\delta\hat{\mathbf{x}}_k := \mathbf{0}_{15\times1}$
  endif
  $\hat{\mathbf{x}}_{k+1} = f_{ins}(\hat{\mathbf{x}}_k, \tilde{\mathbf{u}}_k)$
  $\mathbf{P}_{k+1} = \mathbf{F}_k\mathbf{P}_k\mathbf{F}_k^{\mathrm{T}} + \mathbf{Q}_k$
endloop

4. EXPERIMENTAL RESULTS

Presented data were collected in an office environment with line-of-sight condition to the slaves along the whole trajectory. Four slave units were placed in a rectangle while the navigation unit was swiftly, without turning it, moved counter clockwise in two laps around an 1x1 meter square. The resulting estimated position and slave constellation can be seen in Figure 3, showing the first lap, and Figure 4, showing the second lap. The resulting orientation estimate, for both laps and an initial stationary phase, can be seen in Figure 5. The initial jump to 20° is a mere filter artifact and the concurrent orientation error state estimation error covariance is large. The initial INS state vector, $\mathbf{x}_0$, as well as the error state vector, $\delta\mathbf{x}_0$, were both initialized to zero while the estimation error covariances were initiated to large values. The position as well as the roll and pitch converge swiftly during the initial stationary phase while the yaw starts to converge

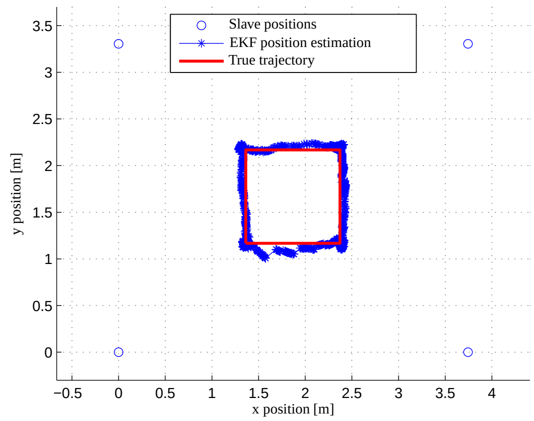

Figure 3: Positioning results from the range aided INS. First lap (counter clockwise) shown with start in the lower left corner. The incorrect orientation estimate at the start and the convergence of the same can clearly be seen in the estimated trajectory of the first (lower) side.

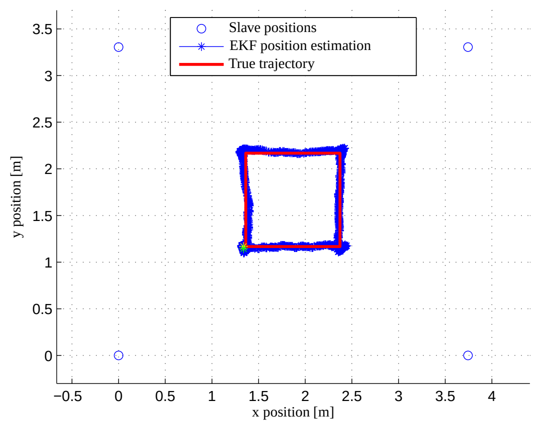

Figure 4: Positioning results from the range aided INS. Second lap shown with start in the lower right corner. The orientation estimate has converged and the error are within 4 cm of the true trajectory.

as soon as there is an acceleration in the horizontal plane and has reached a steady orientation estimate for the second lap. The erroneous orientation estimates during the first lap can clearly be seen, especially along the first (lower), side but also from the bulging appearance of the other sides. This behavior is gone around the second lap for which the orientation has converged. The position discrepancy for the second lap between the estimated and the manually measured trajectory is below 4cm. However, due to difficulties of measuring the exact position of the antennas and the system in motion, the uncertainty of the true trajectory is of about the same order of magnitude. The same holds for the true orientation but the correct behavior of the position estimates around the second lap as in contrast to the first lap indicates that approximately the right yaw has been estimated.

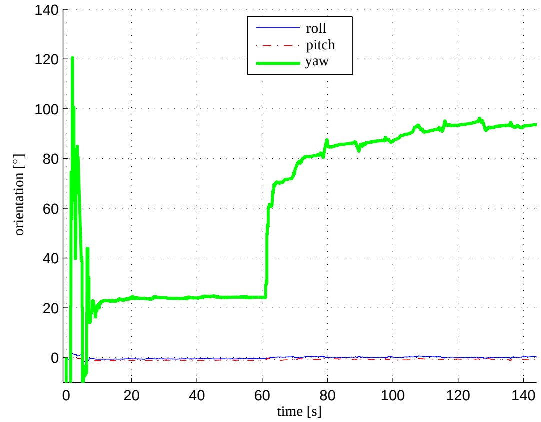

Figure 5: Estimated orientation from the range aided INS. 0-60s is a static phase. The first lap is run over the period of 60-100s and the second lap over 100-140s.

REFERENCES

[1] J. González, J.L. Blanco, C. Galindo, A. Ortiz-de-Galisteo, J.A. Fernández-Madrigal, F.A. Moreno, and J.L. Martínez, "Combination of UWB and GPS for indoor-outdoor vehicle localization", in *Intelligent Signal Processing. WISP 2007. IEEE International Symposium on*, Alcala, Spain, October 3–5. 2007.

[2] E.P. Herrera, R. Quirs, and H. Kaufmann, "Analysis of Kalman approach for a pedestrian positioning system in indoor environments", *Euro-Par 2007 Parallel Processing*, Vol. 4641, pp. 931-940, 2007.

[3] J.A. Corrales, F. A. Candelas, and F. Torres, "Hybrid tracking of human operators using IMU/UWB data fusion by a Kalman filter", *Proc. 3rd ADM/IEEE International Conference on Human-Robot Ineraction*, Amsterdam, Holland, March 12–15. 2008. pp 193-200.

[4] A. De Angelis, J-O. Nilsson, I. Skog, P. Händel, and P. Carbone, "Indoor positioning by ultra wide band radio aided inertial navigation", in *Proc. IMEKO XIV World Congress on Fundamental and Applied Metrology*, Lisbon, Portugal, September 6–11, 2009.

[5] A. De Angelis, M. Dionigi, A. Moschitta, R. Giglietti and P. Carbone, "An experimental UWB distance measurement system", in *Proc. I2MTC 2008, IEEE International Instrumentation and Measurement Technology Conference* , Victoria, BC, Canada, May 12–15, 2008, pp. 1016-1020.

[6] A. De Angelis, M. Dionigi, R. Giglietti and P. Carbone, "Experimental low-cost short pulse generators", in *Proc. I2MTC 2008, IEEE International Instrumentation and Measurement Technology Conference* , Victoria, BC, Canada, May 12–15, 2008, pp. 259-264.

[7] J. Farrell and M. Barth, *The Global Positioning System & Inertial Navigation*, McGraw-Hill, 1999.

[8] A. Chatfield, *Fundamentals of High Accuracy Inertial Navigation*, Reston, 1997.

[9] T. Kailath, A. Sayed, and B. Hassibi, *Linear Estimation*, Prentice-Hall, 2000.